

# Properties of host haloes of Lyman-break galaxies and Lyman-alpha Emitters from their number densities and angular clustering

Takashi Hamana<sup>1,2</sup>, Masami Ouchi<sup>3</sup>, Kazuhiro Shimasaku<sup>3,4</sup>, Issha Kayo<sup>5</sup>  
and Yasushi Suto<sup>4,5</sup>

<sup>1</sup> Institut d’Astrophysique de Paris, 98bis Boulevard Arago, F 75014 Paris, France

<sup>2</sup> National Astronomical Observatory of Japan, Mitaka, Tokyo 181-8588, Japan

<sup>3</sup> Department of Astronomy, School of Science, The University of Tokyo, Tokyo 113-0033, Japan

<sup>4</sup> Research Center for the Early Universe (RESCEU), School of Science, The University of Tokyo, Tokyo 113-0033, Japan

<sup>5</sup> Department of Physics, The University of Tokyo, Tokyo 113-0033, Japan

Accepted \*\*\*\*\*; Received \*\*\*\*\*; in original form 2003 July 10

## ABSTRACT

We explore empirical relations between three different populations of high-redshift galaxies and their hosting dark halos employing the halo model approach. Specifically we consider LBGs (Lyman-break galaxies) at  $z \sim 4$  and at  $z \sim 5$ , and LAEs (Lyman-Alpha emitters) at  $z \simeq 4.86$ , all from the Subaru Deep Field survey extending over an area of about 600 arcmin<sup>2</sup>. We adopt a halo occupation function (HOF) prescription to parameterize the properties of their hosting halos and the efficiency of halo-dependent star formation. We find that the two LBG samples are well described by the halo model with an appropriate HOF. Comparing the model predictions with the observed number densities and the angular correlation functions for those galaxies, we obtain constraints on properties of their hosting halos. A typical mass of hosting halos for LBGs is  $5 \times 10^{11} h^{-1} M_{\odot}$  and the expected number of LBGs per halo is  $\sim 0.5$ , therefore there is an approximate one-to-one correspondence between halos and LBGs. We also find a sign of the minimum mass of LBG hosting halos decreasing with time, although its statistical significance is not strong. We discuss implications of these findings on the star formation history of LBGs. On the other hand, for LAEs, our simple HOF prescription fails to reproduce simultaneously the observed angular correlation function and the number density. In particular, a very high amplitude of the correlation function on scales larger than 120 arcsec cannot be easily reconciled by the HOF model; a set of parameters which account for this high correlation amplitude on large scales predict either excessive clustering on small scales or a much smaller number density than observed. While this difficulty might imply either that the distribution of LAEs within hosting halos differs from that of dark matter, or that the strong large-scale correlation is due to the existence of an unusual, large overdense region, and so the survey region is not a representative of the  $z \sim 5$  universe, the definite answer should wait for a much wider survey of LAEs at high redshifts.

**Key words:** cosmology: theory — galaxies: high redshift — galaxies: haloes — galaxies: formation — dark matter

## 1 INTRODUCTION

Multi-band color selection techniques (Steidel et al. 1996, 1998; Madau et al. 1996; Cowie & Hu 1998; Ouchi et al. 2001, 2003a) have significantly increased high-redshift galaxy catalogs both in quality and in size. Since those high- $z$  galaxies are naturally expected to be progenitors of the present-day galaxies, their statistical analysis is of fundamental impor-

tance in understanding the formation and evolution history of galaxies. Actually, recent large high- $z$  galaxy catalogs allow one to estimate their luminosity functions and spatial correlation functions at different  $z$  with a reasonable accuracy (e.g., Steidel et al. 1999; Adelberger et al. 1998; Giavalisco & Dickinson 2001; Ouchi et al. 2001, 2003a; Porciani & Giavalisco 2002).

In the standard scenario of structure formation, it is

thought that dark matter halos are first formed via the gravitational amplification of initial small density fluctuations. Subsequently baryonic gas trapped in a gravitational potential of the dark matter halo becomes sufficiently dense to cool and to form stars, and such initially small systems experience repeated mergers to form larger galaxies. The formation process of halos is determined by gravity only, thus it is well understood from *N*-body simulations and also from simple but relevant analytical approximations such as the Press-Schechter model (Press & Schechter, 1974) and its extensions (Bond et al. 1991; Bower 1991; Lacy & Cole 1993; Mo & White 1996; Sheth, Mo & Tormen 2001; Sheth & Tormen 2002). The formation of *galaxies*, on the other hand, involves many complicated processes including hydrodynamics, radiative processes, star formation, and supernova feedback, and thus it is hard to solve in a reliable manner even using state-of-the-art numerical simulations. Therefore, a simplified or empirical model that describes essential physical processes is still a valuable tool to understand basic elements of the formation and evolution of galaxies.

This is why we attempt in what follows to apply an empirical parameterized model that relates the galaxy number distribution to mass of the hosting dark matter halo. To be more specific, we explore statistical relations between two populations of high-*z* galaxies and their hosting dark matter halos: (i) Lyman break galaxies (hereafter LBGs) which are isolated in a color–color diagram due to their UV continuum depression (Steidel et al. 1996; 1998; Madau et al. 1996; Adelberger et al. 1998; Ouchi et al. 2001) and (ii) Lyman  $\alpha$  emitters (LAEs) which are identified due to their strong Lyman  $\alpha$  emission from narrow band imaging (Cowie & Hu 1998; Hu, Cowie & McMahon 1998). We consider three catalogs generated from the Subaru Deep Field survey data (Ouchi et al. 2001, 2003a; Shimasaku et al. 2003); LBGs at  $z \sim 4$ , LBGs at  $z \sim 5$  and LAEs at  $z \simeq 4.68$ .

The major purpose of our current analysis is twofold; the first is to clarify the difference of hosting halos for LBGs and LAEs. It is well known that these two populations exhibit different statistical properties, including the fact that LAEs are in general fainter and smaller, and are more strongly clustered than LBGs (Ouchi et al. 2003a). These differences should retain information of their formation processes as well as environmental effects. The second is to examine the difference between LBGs located at different redshifts ( $z \sim 4$  and  $\sim 5$ ). Combined with the previous analysis of LBGs at  $z \sim 3$  by Moustakas & Somerville (2001) and Bullock et al. (2002), our results would provide better understanding of the evolution of LBGs.

For those purposes, we employ the halo approach that attempts to model the spatial distribution of galaxies in a parameterized fashion. The key quantity in this approach is the halo occupation function (HOF) that describes statistical relations between galaxies and their hosting halos. We adopt a simple form for HOF motivated by the semi-analytic galaxy formation models (Benson et al. 2000; Kauffmann et al. 1999) as well as by hydrodynamic simulations (Yoshikawa et al. 2001; White, Hernquist & Springel 2002). Combined with models of the halo mass function and spatial clustering of halos, for which very accurate fitting functions are obtained from *N*-body simulations (Jing 1998; Sheth & Tormen 1999; Hamana et al. 2001; Jenkins et al. 2001), the halo

approach predicts the spatial clustering of galaxies as well as their number density (Mo & Fukugita 1996; Mo, Mao & White 1999). Comparing these predictions with the observed values, we obtain constraints on the relation between galaxies and their hosting halo mass for different populations of galaxies. The latter methodology was first attempted by Jing & Suto (1998) for LBGs at  $z \sim 3$  using their halo catalogs from *N*-body simulations.

The outline of this paper is as follows. Section 2 describes models and basic equations. Section 3 summarizes observational data that are used to put constraints on the model parameters. In section 4, our results of LBGs at  $z \sim 4$  and  $\sim 5$  are presented and are compared with previous results of  $z \sim 3$  LBGs (Moustakas & Somerville 2001; Bullock et al. 2002). We show results of LAEz5, and discuss their implications in section 5. Finally, section 6 is devoted to summary and discussion. In Appendix, we illustrate how the HOF parameters depend on the shape of the two-point correlation function.

Throughout this paper, we adopt a flat  $\Lambda$ CDM (Cold Dark Matter) cosmology with the matter density  $\Omega_m = 0.3$ , the cosmological constant  $\Omega_\Lambda = 0.7$ , the Hubble constant  $H_0 = 100h\text{km/s/Mpc}$  with  $h = 0.7$ , and the normalization of the matter power spectrum  $\sigma_8 = 0.9$ . We adopt the fitting function of the CDM power spectrum of Bardeen et al. (1986).

## 2 HALO APPROACH FOR GALAXY CLUSTERING

The basic idea behind the halo model that we adopt below has a long history (Neyman & Scott 1952; Limber 1953; Peebles 1974, 1980; McClelland & Silk 1977; and other recent papers referred to in this section). The model predictions have been significantly improved with the recent accurate models for the mass function, the biasing and the density profile of dark matter halos (Seljak 2000; Peacock & Smith 2000; Ma & Fry 2000). This approach has been applied to various problems in cosmological nonlinear clustering, galaxy clustering and weak lensing correlation (e.g., Sheth & Jain 1997; Jing, Mo & Börner 1998; Komatsu & Kitayama 1999; Cooray, Hu & Miralda-Escude 2000; Cooray & Sheth 2002; Scoccimarro et al. 2001; Shu, Mao & Mo 2001; Hamana, Yoshida & Suto 2002; Berlind & Weinberg 2002; Bullock, Wechsler & Somerville 2002; Moustakas & Somerville 2002; Takada & Jain 2003; Takada & Hamana 2003). In this section, we summarize several expressions which are most relevant to the current analysis. In particular, we mainly follow the modeling of Berlind & Weinberg (2002), Bullock et al. (2002) and Moustakas & Somerville (2002) in which readers may find further details.

We adopt a simple parametric form for the average number of a given galaxy population as a function of the hosting halo mass:

$$N_g(M) = \begin{cases} (M/M_1)^\alpha & (M > M_{\min}) \\ 0 & (M < M_{\min}) \end{cases} \quad (1)$$

The above statistical and empirical relation is the essential ingredient in the current modeling characterized by the minimum mass of halos which host the population of galaxies ( $M_{\min}$ ), a normalization parameter which can be interpreted

as the critical mass above which halos typically host more than one galaxy ( $M_1$ ; note that  $M_1$  may exceed  $M_{\min}$  since the above relation represents the statistically expected value of the number of galaxies), and the power-law index of the mass dependence of the efficiency of galaxy formation ( $\alpha$ ). We will put constraints on the three parameters from the observed number density and clustering amplitude for each galaxy population. In short, the number density of galaxies is most sensitive to  $M_1$  which changes the average number of galaxies per halo. The clustering amplitude on large angular scales ( $> 1'$ ) is determined by the hosting halos and thus very sensitive to the mass of those halos,  $M_{\min}$ . The clustering on smaller scales, on the other hand, depends on those three parameters in a fairly complicated fashion; roughly speaking,  $M_{\min}$  changes the amplitude,  $\alpha$ , and to a lesser extent  $M_1$  as well, changes the slope (see Appendix). Further detailed discussion may be found in Berlind & Weinberg (2002), Bullock et al. (2002) and Moustakas & Somerville (2002).

With the above relation, the number density of the corresponding galaxy population at redshift  $z$  is given by

$$n_{g,z}(z) = \int_{M_{\min}}^{\infty} dM n_{\text{halo}}(M, z) N_g(M), \quad (2)$$

where  $n_{\text{halo}}(M)$  denotes the halo mass function for which we adopt the fitting function of Sheth & Tormen (1999).

The galaxy two-point correlation function on small scales is dominated by contributions of galaxy pairs located in the same halo. We adopt the following model (Bullock et al. 2002) for the mean number of galaxy pairs  $\langle N_g(N_g - 1) \rangle(M)$  within a halo of mass  $M$ :

$$\langle N_g(N_g - 1) \rangle(M) = \begin{cases} N_g^2(M) & \text{if } N_g(M) > 1 \\ N_g^2(M) \log(4N_g(M))/\log(4) & \text{if } 1 > N_g(M) > 0.25 \\ 0 & \text{otherwise.} \end{cases} \quad (3)$$

The above empirical model is motivated by previous results from the semi-analytic galaxy formation models (Benson et al. 2000; Kauffmann et al. 1999) which indicate that for  $N_g(M) > 1$  the scatter around the mean number of galaxies is Poissonian, while for  $N_g(M) < 1$  it becomes sub-Poissonian.

In the framework of the halo model, the galaxy power spectrum consists of two contributions, one from galaxy pairs located in the same halo (1-halo term) and the other from galaxy pairs located in two different halos (2-halo term):

$$P_g(k) = P_g^{1h}(k) + P_g^{2h}(k). \quad (4)$$

Assuming the linear halo bias model (Mo & White 1996), the 2-halo term reduces to

$$P_g^{2h}(k) = P_{\text{lin}}(k) \times \left[ \frac{1}{n_{g,z}} \int dM n_{\text{halo}}(M) N_g(M) b(M) y(k, M) \right]^2 \quad (5)$$

where  $P_{\text{lin}}(k)$  is the linear dark matter power spectrum,  $b(M)$  is the halo bias factor (we adopt the modified fitting function of Sheth & Tormen 1999), and  $y(k, M)$  is the Fourier transform of the halo dark matter profile normalized by its mass,  $y(k, M) = \tilde{\rho}(k, M)/M$ . See, e.g., section 3 of Seljak (2000) for details. Here we assume that galaxies in

halos trace the density profile of the underlying dark halos by Navarro, Frenk & White (1996; 1997), and adopt the mass-concentration parameter relation by Bullock et al. (2001) but with an appropriate correction (see Shimizu et al. 2003). Since the clustering on large scales is dominated by the 2-halo term, it is fairly insensitive to the assumption of galaxy distribution inside the hosting halo (Berlind & Weinberg 2002). It should be noted that since  $y \simeq 1$  on large scales (e.g., scales much larger than the virial radius of halos), on such scales the 2-halo term can be rewritten by

$$P_g^{2h}(k) = b_g^2(> M_{\min}) P_{\text{lin}}(k) \quad (6)$$

where the galaxy number weighted bias factor is defined by

$$b_g(> M_{\min}) \equiv \frac{\int dM n_{\text{halo}}(M) N_g(M) b(M)}{\int dM n_{\text{halo}}(M) N_g(M)}. \quad (7)$$

Note that  $b_g(> M_{\min})$  depends on  $\alpha$ .

The 1-halo term is written as

$$P_g^{1h}(k) = \frac{1}{(2\pi)^3 n_{g,z}^2} \int dM n_{\text{halo}}(M) \langle N_g(N_g - 1) \rangle(M) \times |y(k, M)|^p. \quad (8)$$

We choose  $p = 2$  for  $\langle N_g(N_g - 1) \rangle > 1$  and  $p = 1$  for  $\langle N_g(N_g - 1) \rangle < 1$  (Seljak 2000). Here we assume that in the limit of a small number of galaxies in one halo, one galaxy is located near the center of the halo. Therefore, in this case, the number of pairs is dominated by the central galaxy paired with a halo galaxy, and thus the probability of finding a galaxy pair is given by the single density profile of the galaxies within a halo.

Once the power spectrum of the galaxy population is specified, one can easily compute their angular two-point correlation function via the Limber projection (see e.g, chapter 2 of Bartelmann & Schneider 2001):

$$\omega(\theta) = \int dr q^2(r) \int \frac{dk}{2\pi} k P_g(k, r) J_0[f_K(r)\theta k], \quad (9)$$

where  $q(r)$  is the normalized selection function and  $J_0(x)$  is the zeroth-order Bessel function of the first kind. For the spatially flat cosmology ( $\Omega_m + \Omega_\Lambda = 1$ ) as we consider throughout the present paper, the radial function  $f_K(r)$  is equivalent to  $r$ , and  $r = r(z)$  is the radial comoving distance given by

$$r(z) = \frac{c}{H_0} \int_0^z \frac{dz}{\sqrt{\Omega_m(1+z)^3 + \Omega_\Lambda}}. \quad (10)$$

The dependences of HOF parameters on the shape of the angular two-point correlation function are summarized in Appendix.

For a given selection function of the observation, the average galaxy number density is

$$n_g = \frac{\int dz \frac{dV(r)}{dz} q(r) n_{g,z}(r)}{\int dz \frac{dV(r)}{dz} q(r)}, \quad (11)$$

where  $dV(r)/dz$  denotes the comoving volume element per unit solid angle:

$$\frac{dV}{dz} = r^2(z) \frac{dr}{dz} = \frac{c}{H_0} \frac{r^2}{\sqrt{\Omega_m(1+z)^3 + \Omega_\Lambda}}, \quad (12)$$

again for the spatially flat cosmology.

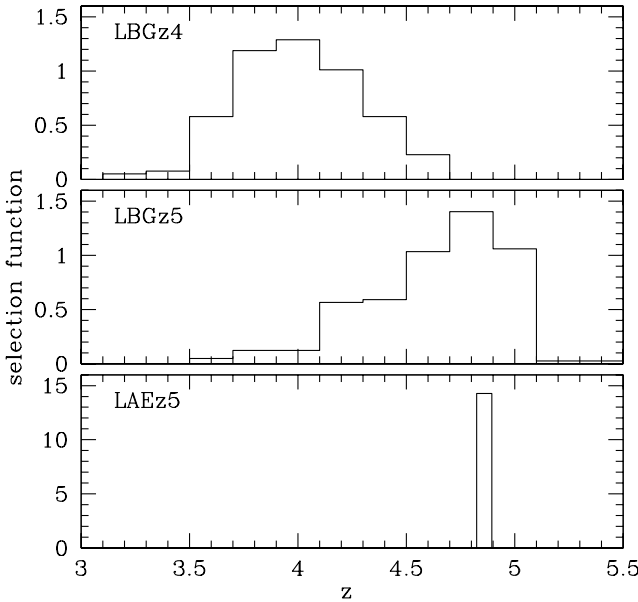


**Figure 1.** Selection functions as a function of redshift for LBGz4 (top), LBGz5 (middle) and LAEz5 (bottom).

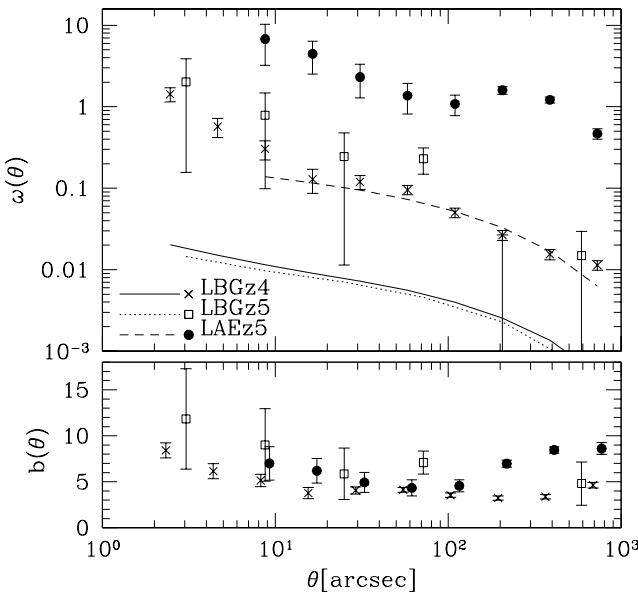


**Figure 2.** Angular two-point correlation functions (upper panel) and the corresponding bias parameter (lower panel) for three populations of high-redshift galaxies. crosses, open squares, and filled circles represent the measured angular two-point correlation functions,  $w_g(\theta)$ , for LBGz4, LBGz5, and LAEz5, respectively. In the lower panel, points for LBGz4 and LAEz5 are slightly shifted horizontally for clarify. The measured correlation functions plotted have been corrected for contamination and for integration constant (see text). The model predictions for dark matter angular two-point correlation functions,  $w_{\text{dm}}(\theta)$ , in the  $\Lambda$ CDM cosmology with the same selection functions are plotted in curves; LBGz4 (solid line), LBGz5 (dotted line) and LAEz5 (dashed line). To compute them, the nonlinear fitting function of the CDM power spectrum by Peacock & Dodds (1996) is used. The biasing parameter is simply defined as  $b(\theta) \equiv \sqrt{w_g(\theta)/w_{\text{dm}}(\theta)}$ .

**Table 1.** Summary of observed properties, here the large scale bias is defined by  $b = \sqrt{w_g/w_{\text{dm}}}$  on scales  $\theta > 100''$ .

Sample	number density [ $h^3 \text{Mpc}^{-3}$ ]	large scale bias
LBGz4	$(5.86 \pm 0.71) \times 10^{-3}$	3 – 4.5
LBGz5	$(8.05 \pm 4.96) \times 10^{-4}$	5 – 7
LAEz5	$(3.01 \pm 1.94) \times 10^{-3}$	5 – 9

### 3 DATA

We use three different samples of galaxy populations from deep imaging data taken as part of the Subaru Deep Field (SDF) survey; LBGs at  $z \sim 4$  (LBGz4s), LBGs at  $z \sim 5$  (LBGz5s) and LAEs at  $z \simeq 4.86$  (LAEz5s). Observational details of those samples are described in Ouchi et al. (2001, 2003a, 2003b), and thus we briefly summarize their basic features relevant for our comparison.

LBGz4s are selected from an  $i'$ -detection catalog constructed from deep  $BRi'$  imaging data over a 543 arcmin $^2$  area in the SDF (Ouchi et al. 2003a). The limiting AB magnitudes for the 3  $\sigma$  detection of an object in a 1''.8 diameter aperture are  $B = 27.8$ ,  $R = 27.1$  and  $i' = 26.9$ . In order to guarantee a reasonable level of photometric completeness, the  $i'$ -detection catalog is limited to  $i' = 26.5$ , corresponding to the absolute magnitude of  $M_{1700} = -19.0 + 5 \log h$  for LBGz4s. A total of 1438 LBGz4 candidates are detected in a range of  $3.5 < z < 4.5$ . The selection function is shown in top-panel of Figure 1, which is estimated using the Monte-Carlo simulation on the basis of colors and redshifts of Hubble Deep Field North galaxies given in the photometric redshift catalog by Furusawa et al. (2000; see Ouchi et al. 2003c, Ouchi 2003 for details).

It should be noted that the selection functions plotted in Figure 1 are the probability distribution functions of galaxy redshifts in our samples. The current observational method does not specify the redshift of individual galaxies accurately except in a statistical sense. Their number density is estimated to be  $n_{\text{LBGz4}} = (5.86 \pm 0.71) \times 10^{-3} h^3 \text{Mpc}^{-3}$ . The angular two-point correlation function is computed by the procedure described in Ouchi et al. (2001; 2003d) and is plotted in Figure 2.

LBGz5s are selected from a  $z'$ -detection catalog constructed from deep  $Vi'z'$  imaging data over a 616 arcmin $^2$  area in the SDF (Ouchi et al. 2003b). The limiting AB magnitudes are  $B = 27.8$ ,  $V = 27.3$ ,  $R = 27.1$ ,  $i' = 26.9$ ,  $z' = 26.1$  for the 3  $\sigma$  detection in a 1''.8 diameter aperture. Again for the photometric completeness, the  $z'$ -detection catalog is limited to  $z' = 26.0$ , corresponding to the absolute magnitude of  $M_{1700} = -19.7 + 5 \log h$  for LBGz5s. A total of 246 LBGz5 candidates are detected in a range of  $4.2 < z < 5.2$ . Their number density is estimated to be  $n_{\text{LBGz5}} = (8.05 \pm 4.96) \times 10^{-4} h^3 \text{Mpc}^{-3}$ .

LAEz5s were first selected from the same data of LBGz5s but an additional observation using a narrow band-filter (NB711, central wavelength of  $7126 \pm 4$  Å, FWHM bandwidth of  $73.0 \pm 0.6$  Å) was performed to identify LAEs at  $z \simeq 4.86$  (Ouchi et al. 2003a). The limiting magnitude is NB711 = 26.0 for the 3  $\sigma$  detection in a 1''.8 diameter aperture. The selection function of LAEz5 is approximated by a top-hat function (bottom-panel of Figure 1) whose shape (center and width) is determined from

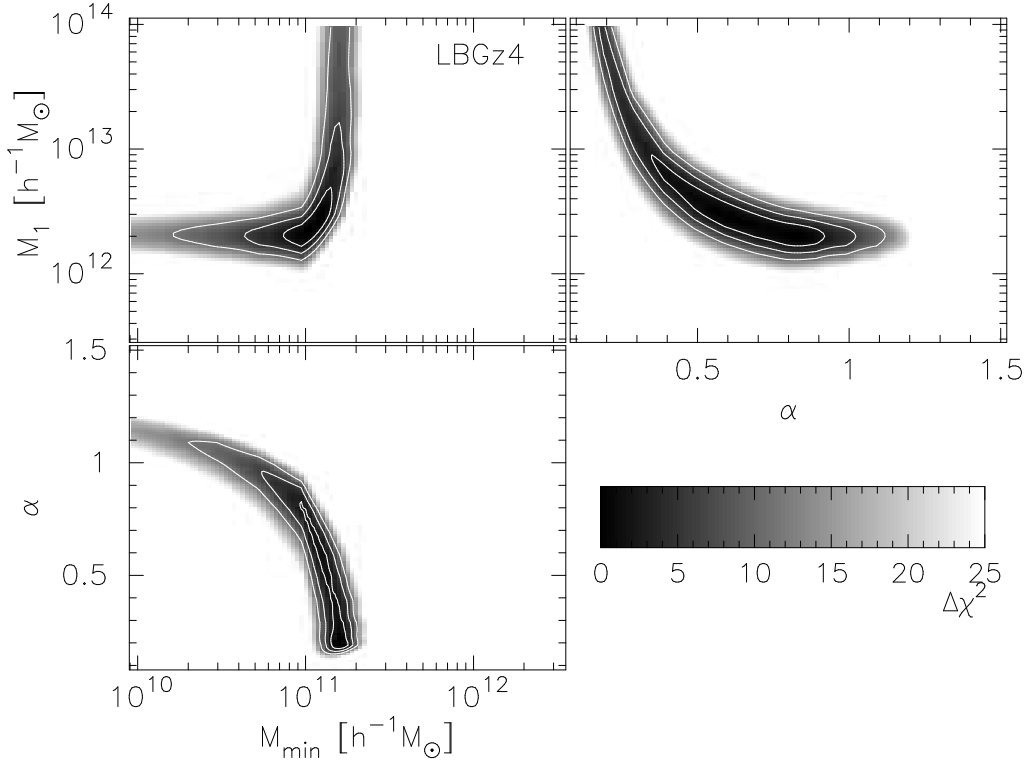


**Figure 3.** Confidence contour maps derived from  $\Delta\chi^2$  for LBGz4 on the two-parameter plane after marginalizing over the remaining one parameter. Top-left panel is on  $M_{\min}$ - $M_1$ , top-right on  $\alpha$ - $M_1$  and bottom-left on  $M_{\min}$ - $\alpha$ . A darker gray-scale indicates a lower  $\Delta\chi^2$  value (thus more likely). Contour lines indicate from inner to outer  $\Delta\chi^2 = 2.3, 6.17$  and  $11.8$ , which, if each bin of the correlation function is independent, correspond to  $68.3, 95.4$ , and  $99.73\%$  confidence levels, respectively. In the present analysis, these confidence levels should be understood as approximate estimates.

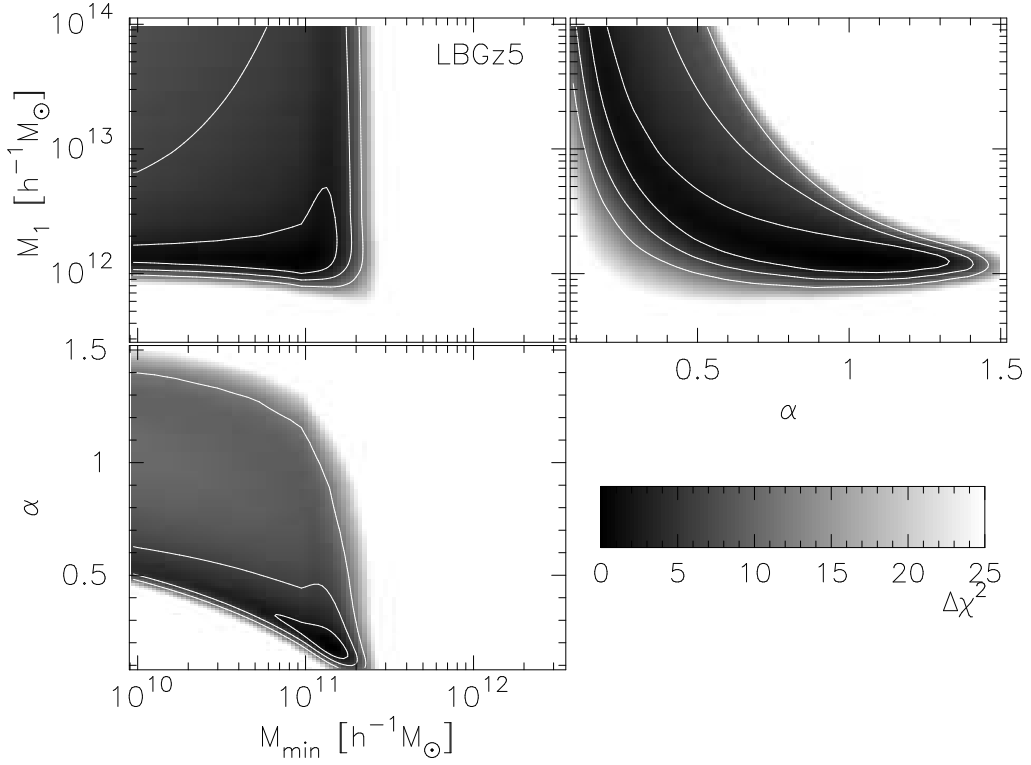


**Figure 4.** Same as Figure 3 but for LBGz5.

the central wavelength and FWHM of the NB711 filter (Ouchi et al. 2003a). A total of 87 LAEz5 candidates are detected over  $4.83 \lesssim z \lesssim 4.89$ . Their number density is  $n_{\text{LAEz5}} = (3.01 \pm 1.94) \times 10^{-3} h^3 \text{Mpc}^{-3}$ .

The angular two-point correlation function  $w_g(\theta)$  for each sample is plotted in Figure 2 together with that for dark matter,  $w_{\text{dm}}(\theta)$ , which is calculated applying the same selection function of the observational data. The plotted correlation functions have been corrected for contamination and for the ‘‘integration constant’’ (see Groth & Peebles 1977). Possible contaminants are mainly low- $z$  galaxies which match the selection criteria by chance, and thus we may safely assume no cross-correlation between high- $z$  LBGs/LAEs and low- $z$  contaminants and no auto-correlation in low- $z$  contaminants. Therefore we have made contamination correction for each sample by multiplying the observed correlation function by a factor of  $1/(1 - f_c)^2$ , where the contamination rate  $f_c$  is estimated to be 0.01, 0.26 and 0.4, for LBGz4s, LBGz5s and LAEz5s, respectively. The integration constant is estimated to be 0.00676, 0.00637 and 0.00675 for LBGz4, LBGz5 and LAEz5, respectively (Ouchi et al. 2001, 2003a, 2003b). We define the biasing parameter as  $b(\theta) \equiv \sqrt{w_g(\theta)/w_{\text{dm}}(\theta)}$ . For LBGs, we obtain large-scale (specifically,  $60'' < \theta < 1000''$ ) bias factors of  $b = 3 - 4.5$  and  $5 - 7$  for LBGz4 and LBGz5s, respectively, and the bias increases with decreasing the separation. On the other hand, LAEs exhibit stronger clustering on larger scales ( $\theta > 200''$ ) than LBGs, while their biases on smaller scales are similar to those of LBGs.

## 4 RESULTS ON LYMAN-BREAK GALAXIES

### 4.1 Constraints on $M_{\text{min}}$ , $M_1$ , and $\alpha$

We estimate the range of allowed values for the three parameters,  $M_{\text{min}}$ ,  $M_1$ , and  $\alpha$  by considering the following  $\chi^2$  function constructed from the observed number density and the angular two-point correlation functions:

$$\chi^2(M_{\text{min}}, M_1, \alpha) = \sum_{\theta_{\text{bin}}} \frac{[\omega^{\text{obs}}(\theta_{\text{bin}}) - \omega^{\text{model}}(\theta_{\text{bin}})]^2}{\sigma_{\omega}^2(\theta_{\text{bin}})} + \frac{[\log n_g^{\text{obs}} - \log n_g^{\text{model}}]^2}{\sigma_{\log n_g}^2}, \quad (13)$$

where  $\sigma_{\omega}$  and  $\sigma_{\log n_g}$  are the statistical  $1-\sigma$  error in the measurements of the angular correlation function and the number density, respectively. In the above likelihood estimator, we take the logarithm of the galaxy number density instead of the number density itself, because the predicted galaxy number density varies logarithmically with  $M_1$ . Note that although the HOF parameters can depend on time in general, we assume here that the three parameters are constant within the redshift interval of each sample for simplicity. For LAEz5s, this must be the case as the redshift interval is very small. It turns out (see §4.3) that the HOF parameters for LBGs do not change significantly over three LBG samples at  $z \sim 3$ ,  $z \sim 4$  and  $z \sim 5$ . Therefore the above assumption is reasonable for LBGs as well. We also note that the present analysis does not take the cosmic variance into account although it may be important for relatively small survey volumes for those samples. Figures 3 and 4 show the  $\chi^2$  map on

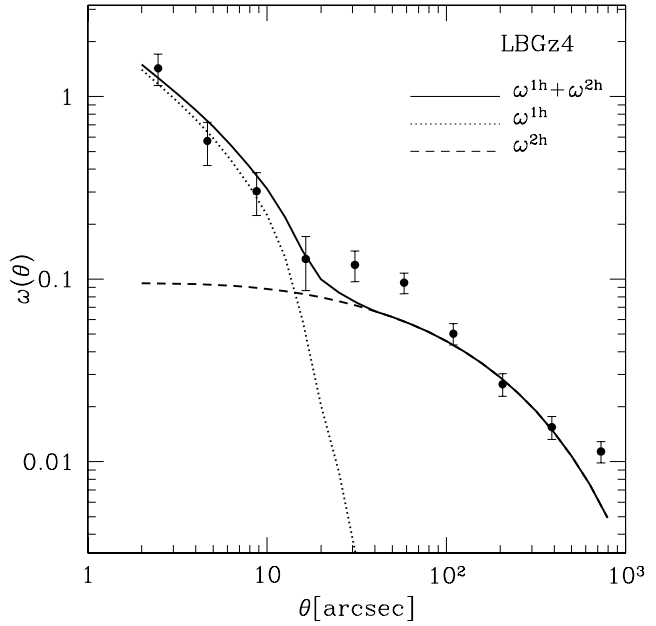


**Figure 5.** Comparison of the observed angular correlation function of LBGz4s with the model prediction assuming  $M_{\text{min}} = 1.6 \times 10^{11} h^{-1} M_{\odot}$ ,  $M_1 = 8 \times 10^{12} h^{-1} M_{\odot}$ , and  $\alpha = 0.75$ .

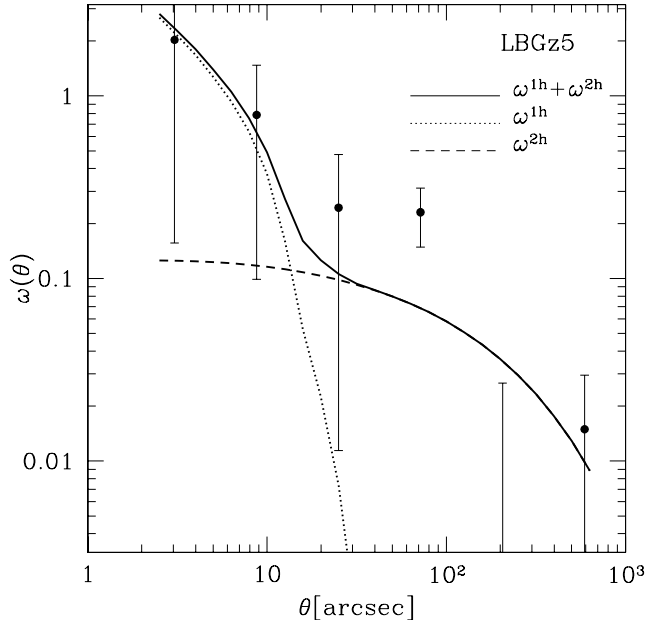


**Figure 6.** Same as Figure 5 but for LBGz5s assuming  $M_{\text{min}} = 1.5 \times 10^{11} h^{-1} M_{\odot}$ ,  $M_1 = 5 \times 10^{12} h^{-1} M_{\odot}$ , and  $\alpha = 0.75$ .

two-parameter planes after marginalizing over the remaining one parameter. The two-dimensional likelihood contours represent  $\Delta\chi^2 = 2.3$ , 6.17 and 11.8 which, if each bin of the correlation function is independent, should correspond to 68.3, 95.4 and 99.7% confidence levels (Press et al. 1986). Strictly speaking, however, the sampled correlation function bins are not completely independent, and these confidence levels should be regarded simply as approximate estimates.

Examine first the parameters for LBGz4s which are fairly strongly constrained by the observations (Fig. 3). Top-

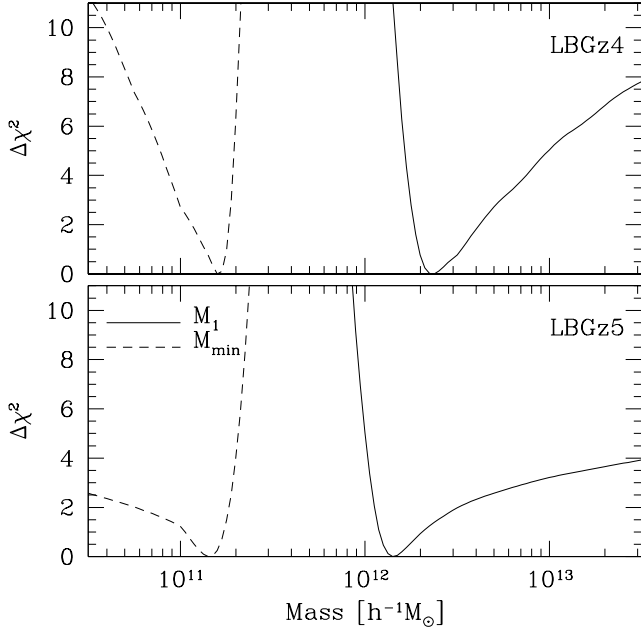


**Figure 7.** The likelihood functions ( $\Delta\chi^2$ ) for  $M_{\min}$  (dashed lines) and for  $M_1$  (solid lines) obtained after marginalizing over the other two parameters. Upper and lower panel is for LBGz4 and LBGz5, respectively.

left panel shows the likelihood map on  $M_{\min}$ - $M_1$  plane. As pointed out earlier by Berlind & Weinberg (2002), Bullock et al. (2002), and Moustakas & Somerville (2002),  $M_1$  and  $M_{\min}$  are mainly constrained by the number density and their clustering amplitude on large scales ( $\theta > 1'$ ), respectively. As Figure 2 shows, the observational uncertainty in the clustering amplitude for LBGz4s is fairly small and  $\delta n/n \sim 12\%$ . Thus we have relatively tight constraints on those two parameters. The constraint on  $\alpha$  is weak because of the degeneracy with the other two parameters. However, it is clear that the data favor  $\alpha < 1$  implying that the galaxy formation is less efficient (or small galaxies merge more efficiently to form larger ones) in more massive halos.

Turn next to LBGz5 (Fig. 4). The constraints on this population are not so tight because of much larger uncertainties in the clustering amplitude (Fig. 2) and in the number density,  $\delta n/n \sim 62\%$ . Nevertheless the constraints on the parameters for LBGz5s seem very similar to those for LBGz4, and we are not able to detect any significant difference of the parameter values of LBGs between  $z = 4$  and 5.

Figures 5 and 6 compare the observed angular two-point correlations with the halo model predictions based on preferred parameters for LBGz4s and LBGz5, respectively. In plotting the model predictions, we adopt  $M_{\min} = 1.6 \times 10^{11} h^{-1} M_\odot$ ,  $M_1 = 8 \times 10^{12} h^{-1} M_\odot$ , and  $\alpha = 0.75$  for LBGz4, and  $M_{\min} = 1.5 \times 10^{11} h^{-1} M_\odot$ ,  $M_1 = 5 \times 10^{12} h^{-1} M_\odot$ , and  $\alpha = 0.75$  for LBGz5. Given the approximate and empirical nature of the halo model, the overall agreement is satisfactory.

**Table 2.** The galaxy-number weighted average mass of hosting halo  $\langle M_{\text{host}} \rangle$  (in units of  $h^{-1} M_\odot$ ) and the expected number of galaxies per one halo  $\langle N_g \rangle$  for typical values of HOF parameters.

Sample ( $M_{\min}$ , $M_1$ , $\alpha$ )	$\langle N_g \rangle$	$\langle M_{\text{halo}} \rangle$
LBGz4 ( $1.6 \times 10^{11}$ , $2.4 \times 10^{12}$ , 0.5)	0.38	$6.3 \times 10^{11}$
LBGz5 ( $1.4 \times 10^{11}$ , $1.4 \times 10^{12}$ , 0.5)	0.45	$4.5 \times 10^{11}$

#### 4.2 Characteristics of LBG hosting halos

Let us look into more carefully the hosting halo masses for the two LBG samples. Figure 7 plots the likelihood functions ( $\Delta\chi^2$ ) for  $M_{\min}$  (dashed lines) and for  $M_1$  (solid lines) after marginalizing over the remaining two parameters. Clearly, both likelihood functions look similar, indicating little evolution of properties of the hosting halos from  $z \sim 5$  to  $z \sim 4$ .

In order to estimate the characteristic mass of hosting halos and the typical number of galaxies per halo, we introduce the following two quantities: the average mass of the hosting halo (member galaxy number weighted):

$$\langle M_{\text{host}} \rangle = \frac{\int_{M_{\min}}^{\infty} dM M N_g(M) n_{\text{halo}}(M)}{\int_{M_{\min}}^{\infty} dM N_g(M) n_{\text{halo}}(M)}, \quad (14)$$

and the average number of galaxies per halo:

$$\langle N_g \rangle \equiv \frac{\int_{M_{\min}}^{\infty} N_g(M) n_{\text{halo}}(M, z) dM}{\int_{M_{\min}}^{\infty} n_{\text{halo}}(M, z) dM}. \quad (15)$$

Those are evaluated assuming typical sets of HOF parameters that we found in the previous subsection (Table 2). The average mass of the hosting halos for LBGs is  $(5-6) \times 10^{11} h^{-1} M_\odot$ , and the average number of galaxies per halo is  $\sim 0.4$ . Thus LBGs have an approximate one-to-one correspondence to relatively less massive halos.

#### 4.3 Evolution of properties of the hosting halos for LBGs

Turn next to the evolution of the hosting halos for LBGs. Our current analysis indicates that the minimum halo mass  $M_{\min}$  for LBGs is almost the same  $\sim 1.5 \times 10^{11} h^{-1} M_\odot$  at  $z \sim 4$  and  $z \sim 5$ . The halo mass accommodating more than one galaxy,  $M_1$ , seems increasing as time although barely at a  $1-\sigma$  level.

The almost identical analyses by Moustakas & Somerville (2001) and Bullock et al. (2002) for  $z \sim 3$  LBGs (Steidel et al. 1998; Adelberger et al. 1998; Adelberger 2000) indicate that  $M_{\min} = 1.3 \times 10^{10} h^{-1} M_\odot$  and  $M_1 = 6 \times 10^{12} h^{-1} M_\odot$  for  $\alpha = 0.8$ , and that  $M_{\min} = (0.4-8) \times 10^{10} h^{-1} M_\odot$ ,  $M_1 = (6-10) \times 10^{12} h^{-1} M_\odot$  and  $0.9 < \alpha < 1.1$ , respectively. Taking account of the relatively large uncertainties in those estimates, their results are consistent with ours, and indeed the combined results may indicate an evolutionary trend of decreasing  $M_{\min}$  and increasing  $M_1$  with decreasing  $z$ . The different selection criteria at different redshifts may induce an artificial systematic effect in estimating hosting halo mass, but this is not the case here. If the limiting flux of a sample is brighter, galaxies in the sample have a smaller number density and usually a higher clustering amplitude. This leads to increasing  $M_{\min}$  and  $M_1$  simultaneously. However, the limiting ab-

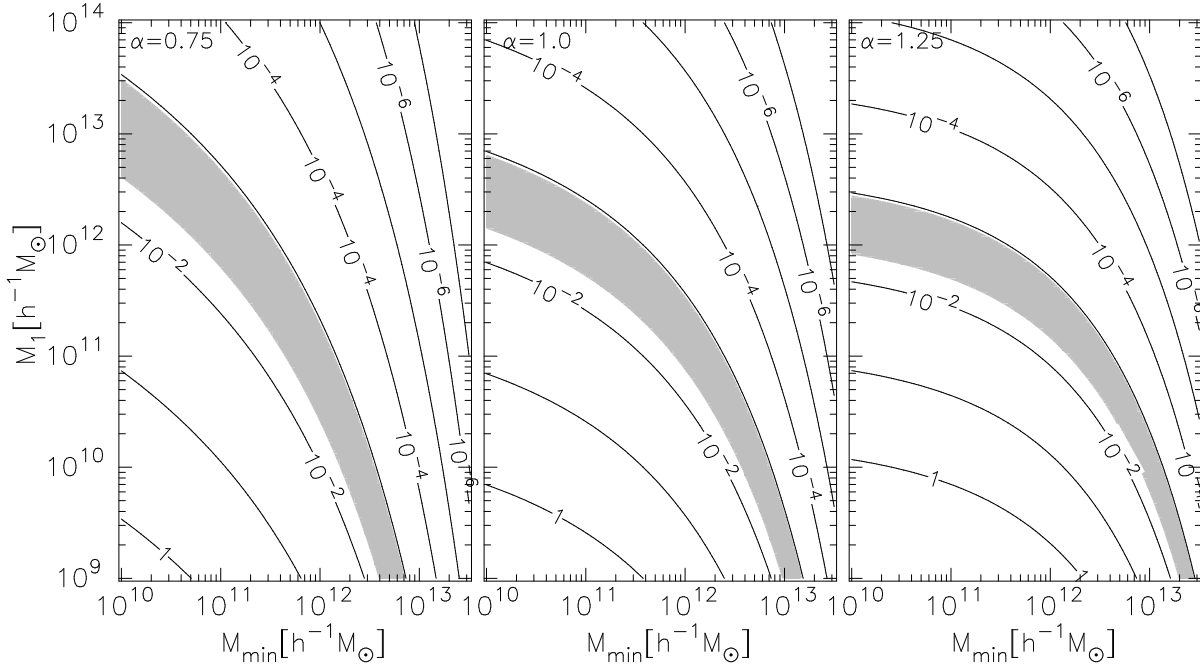


**Figure 8.** Contours show the halo model prediction for the number density of LAEz5s. Grayed region shows the  $1-\sigma$  range of the observed value of  $n_g = (3.01 \pm 1.94) \times 10^{-3} (h \text{Mpc}^{-1})^3$ . Form left to right  $\alpha = 1.25, 1.0$  and  $0.75$ , respectively.

solute magnitudes for LBGz3s, LBGz4s and LBGz5s are  $M_{1700} = -19.3 + 5 \log h$ ,  $M_{1700} = -19.0 + 5 \log h$  and  $M_{1700} = -19.7 + 5 \log h$ , respectively. Therefore, it is very unlikely that the difference in the limiting magnitude solely accounts for the systematic (although weak) trends in  $M_{\min}$  and  $M_1$ .

In summary, the hosting halos for LBGs are characterized as follows; (i)  $M_{\min}$  is about  $\simeq 1.5 \times 10^{11} h^{-1} M_\odot$  both at  $z \sim 4$  and  $z \sim 5$ , while it decreases to about  $M_{\min} = (0.4-8) \times 10^{10} h^{-1} M_\odot$  at  $z \sim 3$ . (ii)  $M_1$  increases with time,  $M_1 \simeq 1.4 \times 10^{12}, 2.4 \times 10^{12}$  and  $(6-10) \times 10^{12} h^{-1} M_\odot$  for  $z = 5, 4$  and  $3$ , respectively.

## 5 RESULTS ON LYMAN-ALPHA EMITTERS

Let us turn to LAEz5s. As shown in Figure 2, their angular correlation function exhibits a somewhat irregular shape. This is more clearly seen in the plot of the bias (lower panel of Figure 2). On scales less than 120 arcsec, the bias increases with decreasing separation similarly to LBGs, and its amplitude is in the range between those for LBGz4s and LBGz5s. On the other hand, on larger scales the bias factor is rather high, which is in a marked contrast with LBGs. The number density of LAEs is higher than that of LBGz5s but it has a large uncertainty,  $\delta n/n \sim 65\%$ . It should be noted that the survey volume of LAEz5 is small,  $(30 h^{-1} \text{Mpc})^3$  (comoving volume), thus it is possible that these measurements are significantly affected by the cosmic variance.

For reference, we give here some numbers which are useful in the following discussion; at the redshift of LAEz5s,  $z \simeq 4.86$ , 1 arcmin corresponds to  $1.56 h^{-1} \text{Mpc}$  (comoving), and the average number of halos with the mass larger than  $M$  within the survey volume computed from the halo mass

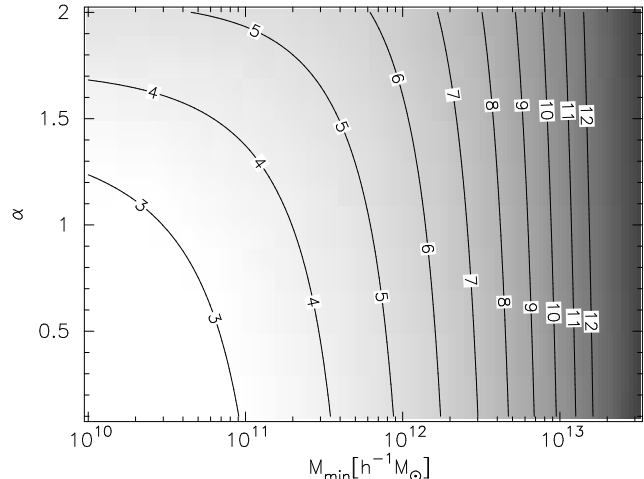


**Figure 9.** Contours show the halo model prediction for the galaxy number weighted large scale bias factor defined by eq. (6).

function is  $N(> M) = 90, 10$  and  $1$ , for  $M = 3 \times 10^{11}, 1 \times 10^{12}$ , and  $3 \times 10^{12} h^{-1} M_\odot$ , respectively.

We apply the same likelihood analysis as performed for LBGs in the last section, but we find that our simple HOF prescription fails to reproduce simultaneously the observed angular correlation function and number density. Indeed, no parameter set is found to give a reasonably small  $\chi^2$ . The most serious discrepancy is the very high correlation amplitude on scales larger than 120 arcsec. In what follows, we present two illustrative examples of failed models, which would help to search for a possible solution of the problem. For this purpose, we plot halo model predictions for the number density of LAEz5s in Figure 8, in which the

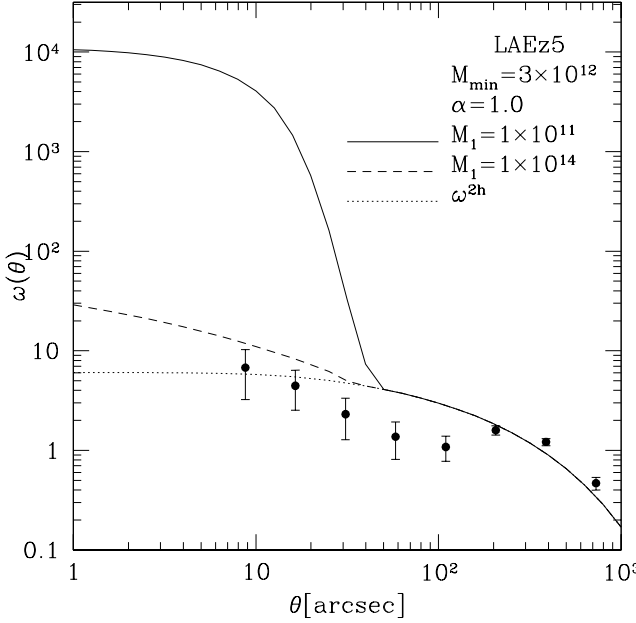


**Figure 10.** Comparison of the observed angular correlation function of LAEz5 with the model prediction assuming  $\alpha = 1.0$ ,  $M_{\min} = 3.0 \times 10^{12} h^{-1} M_\odot$  and  $M_1 = 1 \times 10^{11} h^{-1} M_\odot$  for the solid line, and  $M_1 = 1 \times 10^{14} h^{-1} M_\odot$  for the dashed line. The dotted line shows the 2-halo term only which does not depends on  $M_1$ .

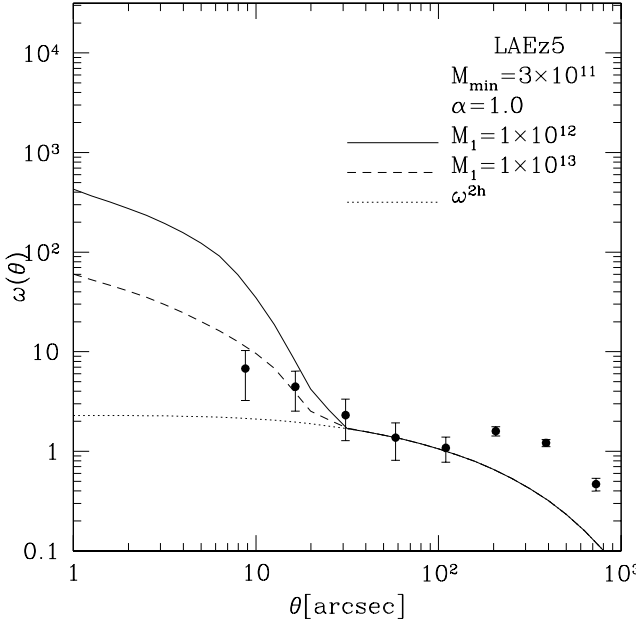


**Figure 11.** Same as Figure 10 but for different HOF parameter sets  $M_{\min} = 3.0 \times 10^{11} h^{-1} M_\odot$ ,  $\alpha = 1.0$ , and  $M_1 = 1.0 \times 10^{12}$  (the solid line) and  $10^{13}$  (dashed line).

gray region indicates the  $1-\sigma$  range of the observed number density, and halo model predictions for the large scale bias factor defined by eq. (6) in Figure 9.

The first example is as follows; taking the amplitude of the correlation function on large scales ( $b = 7-9$  for  $\theta > 120$  arcsec, see Figure 2), one finds in Figure 9 that  $M_{\min} =$

$(2-5) \times 10^{12} h^{-1} M_\odot$  is required irrespective of  $\alpha$ . This value combined with the observed number density of LAEz5s gives roughly  $M_1 \sim 10^{11} h^{-1} M_\odot$  (or less) for a reasonable range of  $\alpha$  (Fig. 8). This parameter set, however, predicts a much higher correlation amplitude than observed on smaller scales (Fig. 10). If one attempts to have a reasonable correlation amplitude on smaller scale, a very large  $M_1$  (more than  $\sim 10^{14} h^{-1} M_\odot$  at least) is required (see Fig. 10), which leads to too small a number density on the other hand.

One possible way to reconcile this discrepancy is to modify the halo model that we have adopted. Figure 10 indicates that it is the 1-halo term that boosts the correlation amplitude on smaller scales. Therefore, our assumption in the halo model that the galaxy distribution follows the dark matter distribution may not hold for LAEz5s. In this paper, however, we do not attempt to develop the HOF model by allowing a possible variation on the galaxy distribution within halos, because the statistical accuracies of the correlation functions on small scales are still relatively low. Indeed, the number of small separation pairs is very small; the number of LAE pairs which fall into the smallest separation bin is two, and that into the second bin is five. This means that halos having more than one LAE are limited, and one has to keep in mind that the correlation function measurements on these scales are based on LAEs in such a small number of halos. Given a possible large uncertainty in the measurements of small-scale clustering, it is premature to explore an alternative model in great detail at this point. We also note that given the limited number of LAEz5s, it is not to be denied that their correlation signals are contaminated by the presence of the possible foreground galaxies in one or a few clusters. We must wait for future data extending over a much larger survey area.

In addition to the above problem, there is another problem concerning the predicted number of halos in the survey volume. If one takes  $M_{\min} = 3 \times 10^{12} h^{-1} M_\odot$ , the expected mean number of halos with mass larger than this value in the survey volume is  $N(> 3 \times 10^{12} h^{-1} M_\odot) \sim 1$ . This suggests that there are only a few hosting halos in the survey volume. If this picture is right, it is unlikely that the 2-halo term is correctly measured from such a small number of halos.

The above consideration implies that a simple halo model may not be readily applicable to the LAEs. Note that the parameter set  $(M_{\min}, M_1, \alpha) = (3 \times 10^{12} h^{-1} M_\odot, 1 \times 10^{11} h^{-1} M_\odot, 1.0)$  gives  $\langle N_g \rangle = 45$  and  $\langle M_{\text{halo}} \rangle = 5.2 \times 10^{12} h^{-1} M_\odot$ . Therefore, if real, we can conclude at least that the nature of hosting halos and the relation between galaxies and halos for LAEs are very different from those for LBGs.

The second example is as follows. Let us ignore the data on large scales ( $\theta > 120$  arcsec) for a while, and adopt the value of  $b$  around 1 arcmin, i.e.,  $b \simeq 4$ . This gives  $M_{\min} = (2-4) \times 10^{11} h^{-1} M_\odot$  (Fig. 9). This value combined with the observed number density gives roughly  $M_1 \sim 10^{12} h^{-1} M_\odot$  for a reasonable range of  $\alpha$  (Fig. 8). This parameter set predicts a slightly higher correlation amplitude on small scales than observed as shown in Figure 11. However, this discrepancy may not be taken so seriously, because of the limited statistical significance as mentioned above. Better agreement is obtained by setting larger  $M_1 \sim 10^{13} h^{-1} M_\odot$  (Fig. 11), which, however, predicts a smaller number density than observed. The discrepancy in the number density becomes

smaller if one takes a smaller  $\alpha$  (Fig. 8). If we take  $(M_{\min}, M_1) = (3 \times 10^{11} h^{-1} M_\odot, 1 \times 10^{12} h^{-1} M_\odot)$ , the characteristic values are  $\langle N_g \rangle = 0.67$  and  $\langle M_{\text{halo}} \rangle = 9.0 \times 10^{11} h^{-1} M_\odot$  for  $\alpha = 0.75$ , and  $\langle N_g \rangle = 0.75$  and  $\langle M_{\text{halo}} \rangle = 7.8 \times 10^{11} h^{-1} M_\odot$  for  $\alpha = 0.5$ . These values are similar to those for LBGs.

The above model provides acceptable agreement with both the correlation function on scales smaller than 120 arcsec and the number density. The predicted correlation function on larger scales, however, has a much lower amplitude than observed. A possible interpretation to this discrepancy is that the current survey volume is one of the overdense regions on large scales by chance, and the LAEs in the region have accidentally acquired the high correlation amplitude. In fact, Shimasaku et al. (2003) have extended the survey area of LAEz5s to the north and found a high overdensity of LAEz5s over a circular region of 5 arcmin ( $8h^{-1}\text{Mpc}$ ) radius. They have suggested that it may be a progenitor of a present-day massive cluster of galaxies. Half of this circular region is inside our survey area. LAEz5s associated with this large-scale overdense region will have an unusually high correlation amplitude on large scales. If this is the case, the HOF parameter values obtained ignoring the large-scale correlation function will be close to the typical values of LAEs at  $z \sim 5$ .

## 6 SUMMARY AND DISCUSSIONS

We have analyzed three high-redshift galaxy samples created from the Subaru Deep Field (SDF) survey data; LBGs at  $z \sim 4$  (LBGz4s), LBGs at  $z \sim 5$  (LBGz5s) and LAEs at  $z \simeq 4.86$  (LAEz5s), and explored the implications of their number density and angular clustering in the framework of the halo occupation function (HOF).

Our major findings are summarized as follows;

(i) The two LBG samples can be well described by the halo model with an appropriate HOF in an approximate fashion.

(ii) The hosting halos for LBGz4s and LBGz5s are more massive than  $M_{\min} \sim 1.5 \times 10^{11} h^{-1} M_\odot$ . Since the expected number of LBGs per halo with  $M > M_{\min}$  is  $\sim 0.5$ , there is an approximate one-to-one correspondence between halos and LBGs. This is basically consistent with the results previously found for LBGs at  $z \sim 3$  (Mo, Fukugita 1996; Steidel et al. 1998; Jing & Suto 1998; Moustakas & Somerville 2001; Berlind & Weinberg 2002; Bullock et al. 2002).

(iii) On the other hand, this may also indicate that a large fraction of dark halos do not host LBGs brighter than  $M_{1700} \simeq -19$  mag. Nevertheless this does not necessarily mean that there is no galaxy in such halos. Franx et al. (2003) have found a population of red galaxies at  $z \sim 3$  which do not have active star formation and so may not be easily detectable by the Lyman break technique because of the very faint UV continuum emission. They estimate that the number density of such red galaxies is about half that of LBGs at the same redshift. Thus it may be the case that a fraction of the dark halos at  $z \sim 4-5$  host such red galaxies rather than bright LBGs that we have discussed here.

(iv) The LBG samples at  $z \sim 3, 4$  and  $5$  discussed here have very similar limiting absolute magnitudes,  $M_{1700} \simeq -19$ . On the other hand, the minimum mass of their hosting halos seems decreasing with time, although its statistical

significance is not strong. If true, this means that the star formation efficiency per unit dark matter mass,  $L_{1700}/M_{\text{halo}}$ , increases with time. This increase may suggest that cold gas gradually accumulates in LBGs, if the star formation rate is simply proportional to the amount of cold gas.

(v) There is a weak indication for  $M_1$  to increase slightly with time in the LBG samples. If this is indeed the case, it may be explained by the mutual merging of LBGs.

(vi) For LAEz5s, our simple HOF prescription fails to reproduce simultaneously the observed angular correlation function and number density. No parameter set gives a reasonably small  $\chi^2$ . This is mainly because the LAEz5s exhibit very strong clustering signal on scales larger than 120 arcsec.

In fact, the nature of LAEz5s is still uncertain in the current result; models which match both the high correlation amplitude on large scales and the number density of LAEz5s predict much higher correlation amplitude on small scales than observed. A possible interpretation of this discrepancy is that the distribution of LAEs within halos differs from that of dark matter. If this is the case, the simple halo model description for the LAE we adopted in this paper needs to be improved. Also the observational indication for the discrepancy should be carefully confirmed with future larger and more accurate data samples.

Alternatively, if one constructs models which match both the correlation function on small scales and the number density of LAEz5s, they imply a lower correlation amplitude on large scales than observed. This may be simply due to statistical fluctuation in a sense that the current data do not represent a fair sample of the universe at  $z \sim 5$  as indicated by Shimasaku et al. (2003). The HOF parameters derived from the fit to the observed data except for the large scale correlation function are  $M_{\min} \sim 3 \times 10^{11} h^{-1} M_\odot$  and  $M_1 \sim 1 \times 10^{12} h^{-1} M_\odot$  for a reasonable range of  $\alpha$ . This gives  $\langle N_g \rangle \sim 0.7$  and  $\langle M_{\text{halo}} \rangle \sim 8 \times 10^{11} h^{-1} M_\odot$  for  $\alpha = 0.75$ , suggesting an approximate one-to-one correspondence between LAEs and halos as found for LBGs.

In order to distinguish the above two pictures, we need a much larger observational sample after all.

## ACKNOWLEDGMENTS

T.H. and M.O. acknowledge support from Japan Society for Promotion of Science (JSPS) Research Fellowships. I. K. gratefully acknowledges support from the Takenaka-Ikueikai fellowship. This research was also supported in part by the Grants-in-Aid from Monbu-Kagakusho and Japan Society of Promotion of Science (12640231, 13740150, 14102004, and 1470157). Numerical computations presented in this paper were carried out at ADAC (the Astronomical Data Analysis Center) of the National Astronomical Observatory, Japan (project ID: mys02a, yys08a).

## REFERENCES

Adelberger K. L., 2000, in ASP Conf. Ser. 200, Clustering at High Redshift, ed. A. Mazure, O. Le Févre, & V. Le Brun (San Francisco: ASP), 13  
 Adelberger K. L., Steidel C. C., Giavalisco M., Dickinson M., Pettini M., Kellogg M., 1998, ApJ, 505, 18

Bardeen J. M., Bond J. R., Kaiser N., Szalay A. S. 1986, ApJ, 304, 15

Bartelmann M., Schneider P., 2001, Phys. Rep., 340, 291

Benson A. J., Cole S., Frenk C. S., Baugh C. M., Lacey C. G., 2000, MNRAS, 311, 793

Berlind A. A., Weinberg D. H., 2002, ApJ, 575, 587

Bond J. R., Cole S., Efstathiou G., Kaiser N., 1991, ApJ, 379, 440

Bower R. G., 1991, MNRAS, 248, 332

Bruzual A. G., Charlot, S., 1993, ApJ, 405, 538

Bullock J. S., Kolatt T. S., Sigad Y., Somerville R. S., Kravtsov A. V., Klypin A. A., Primack J. R., Dekel A. 2001, MNRAS, 321, 559

Bullock J. S., Wechsler, R. H., Somerville R. S., 2002, MNRAS, 329, 346

Cooray A., Hu W., Miralda-Escude J. 2000, ApJ, 535, L9

Cooray A., Sheth R., 2002, Phys. Rep., 372, 1

Cowie L. L., Hu E. M., 1998, AJ, 115, 1319

Furusawa, H., Shimasaku, K., Doi, M., Okamura, S., 2000, ApJ, 534, 624

Franx, M. et al., 2003, ApJ, 587, L79

Giavalisco M., Dickinson M., 2001, ApJ, 550, 177

Hamana T., Yoshida N., Suto Y., 2002, ApJ, 568, 455

Hamana T., Yoshida N., Suto Y., Evrard A. E., 2001, ApJ, 561, L143

Hu E. M., Cowie L. L., McMahon R. G., 1998, ApJ, 502, L99

Jenkins A., Frenk C. S., White S. D. M., Colberg J. M., Cole S., Evrard A. E., Couchman H. M. P., Yoshida N., 2001, MNRAS, 321, 372

Jing Y. P., 1998, ApJ, 503, L9

Jing Y. P., Mo H. J. Böner G., 1999, ApJ, 494, 1

Jing Y. P., Suto Y., 1998, ApJ, 494, L5

Kauffmann G., Colberg J. M., Diaferio A., White, S. D. M., 1999, MNRAS, 303, 188

Komatsu E., Kitayama T. 1999, ApJ., 526, L1

Lacey C., Cole S. 1993, MNRAS, 262, 627

Limber D. N. 1953, ApJ, 117, 134

Ma C.-P., Fry J. N. 2000, ApJ, 543, 503

Madau P., Ferguson H. C., Dickinson M. E., Giavalisco M., Steidel C. C., Fruchter A., 1996, MNRAS, 283, 1388

Malhotra, S. & Rhoads, J. E. 2002, ApJ, 565, L71

McClelland J., Silk J. 1977, ApJ, 217, 331

Mo, H. J., Fukugita, M. 1996, ApJ, 467, L9

Mo, H. J., Mao, S., White, S. D. M. 1999, MNRAS, 304, 175

Mo, H. J., White, S. D. M. 1996, MNRAS, 282, 347

Moustakas L. A., Somerville R. S., 2002, ApJ, 577, 1

Navarro J., Frenk C., White S. D. M. 1996, ApJ, 462, 563

Navarro J., Frenk C., White S. D. M. 1997, ApJ, 490, 493

Neyman J., Scott E. L. 1952, ApJ, 116, 144

Ouchi, M. 2003, Ph.D. Thesis, University of Tokyo

Ouchi M., et al., 2001, ApJ, 558, L83

Ouchi M., et al., 2003a, ApJ, 582, 60

Ouchi M., et al., 2003b, Carnegie Observatories Astrophysics Series, Vol. 3: Clusters of Galaxies: Probes of Cosmological Structure and Galaxy Evolution , ed. J. S. Mulchaey, A. Dressler, and A. Oemler (Pasadena: Carnegie Observatories, <http://www.ociw.edu/ociw/symposia/series/symposium3/proceedings.html>)

Ouchi M., et al., 2003c, ApJ submitted (astro-ph/0309655)

Ouchi M., et al., 2003d, ApJ submitted (astro-ph/0309657)

Peacock J. A., Dodds S. J., 1996, MNRAS, 280, L19

Peacock J. A., & Smith R. E. 2000, MNRAS, 318, 1144

Peebles P. J. E. 1974, A&A, 32, 197

Peebles P. J. E., 1980, The Large-Scale Structure of the Universe Princeton Univ. Press, Princeton, NJ

Porciani C., Giavalisco M., 2002, ApJ, 565, 24

Press W. H., Flannery B. P., Teukolsky S. A., Vetterling W. T., 1986, Numerical Recipes (Cambridge: Cambridge Univ. Press)

Press W. H., Schechter P., 1974, ApJ, 187, 425

Schaerer D., 2003, A&A, 397, 527

Scoccimarro R., Sheth R. K., Hui L., Jain B., 2001, ApJ, 546, 20

Seljak U. 2000, MNRAS, 318, 203

Sheth R. K., Jain B.. 1997, MNRAS, 285, 231

Sheth R. K., Mo. H. J., Tormen G., 2001, MNRAS, 323, 1

Sheth R. K., Tormen G., 1999, MNRAS, 308, 119

Sheth R. K., Tormen G., 2002, MNRAS, 329, 61

Shimasaku K. et al., 2003, ApJ, 586, L111

Shimizu, M., Kitayama, T., Sasaki, S., Suto, Y., 2003, ApJ, 590, 197

Shu, C., Mao, S., Mo, H. J., 2001, MNRAS, 327, 895

Steidel C. C., Giavalisco M., Pettini M., Dickinson M., Adelberger K. L., 1996, ApJ, 461, L17

Steidel C. C., Adelberger K. L., Dickinson M., Giavalisco M., Pettini M., Kellogg M., 1998, ApJ, 492, 428

Steidel C. C., Adelberger K. L., Giavalisco M., Dickinson M., Pettini M., 1999, ApJ, 519, 1

Takada M., Hamana T., 2003, MNRAS in press (astro-ph/0305381)

Takada M., Jain B., 2003, MNRAS, 340, 580

White M., Hernquist L., Springel V., 2002 ApJ, 580, 634

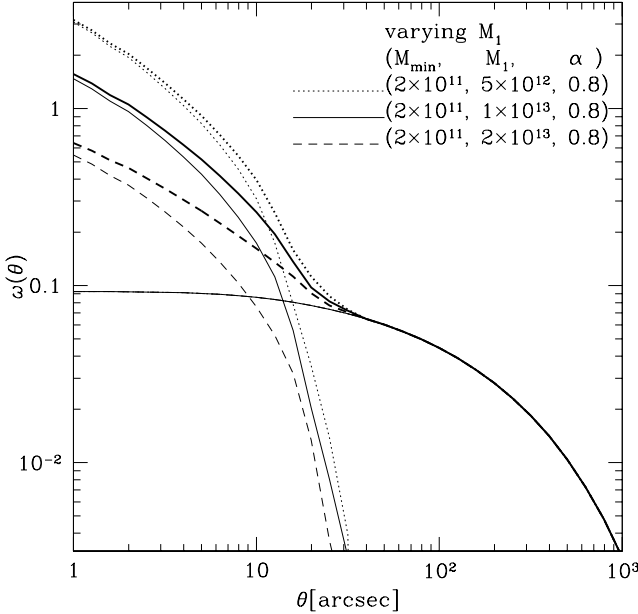
Yoshikawa K., Taruya A., Jing Y.-P., Suto Y., 2001, ApJ, 558, 520

## APPENDIX A: DEPENDENCES OF HOF PARAMETERS ON THE SHAPE OF THE TWO-POINT CORRELATION FUNCTION

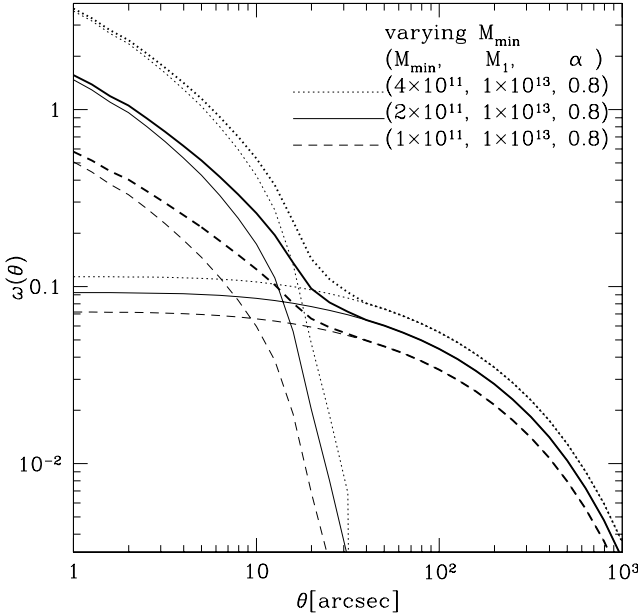
Here we summarize major characteristics of changes in the shape of the two-point correlation functions made by varying HOF parameters. Figure A1-A3 show the angular correlation functions for variety of HOF models. Each Figure demonstrates the effect of varying one HOF parameter with fixing other two parameters. In all plots, the selection function of LBGz4 is adopted for an illustrative purpose. It should be noticed that a degree of change in the shape of the correlation function made by varying one parameter depends on a choice of other two parameters, thus the plots should be understood as illustrative examples, and we just focus on major characteristics from a qualitative point of view.

Figure A1 shows the effect of varying  $M_1$  on  $\omega$ . Since the 2-halo term does not depend on  $M_1$ , the correlation function on larger scales is not affected by the change of  $M_1$ . The amplitude of the 1-halo term decreases with increasing  $M_1$ . This is mainly due to the decrease in the contribution from smaller mass halos.

Figure A2 is for effect of varying  $M_{min}$ . The amplitude of the 2-halo term increases with  $M_{min}$ , because of a larger



**Figure A1.** Dependence of varying  $M_1$  on the shape of angular two-point correlation functions. HOF parameters for three cases are inserted in the plot. Two thin lines show 1-halo (dominates on small scales) and 2-halo term (dominates on large scales) and thin lines show the sum of them. We take the selection function of LBGz4 to compute those correlation functions for an illustrative purpose.



**Figure A2.** Same as Figure A1, but for  $M_{\min}$ .

bias factor for more massive halos. The amplitude of the 1-halo term also increases with  $M_{\min}$ . This is largely the decrease in the contribution from smaller mass halos.

Finally Figure A1 shows the effect of varying  $\alpha$  on  $\omega$ . Varying  $\alpha$  changes the fraction of galaxies in massive halo to less massive halos. A larger  $\alpha$  gives more weight for galaxies in massive halos. Since a stronger bias factor for more massive halo, a larger  $\alpha$  gives a larger amplitude of the 2-

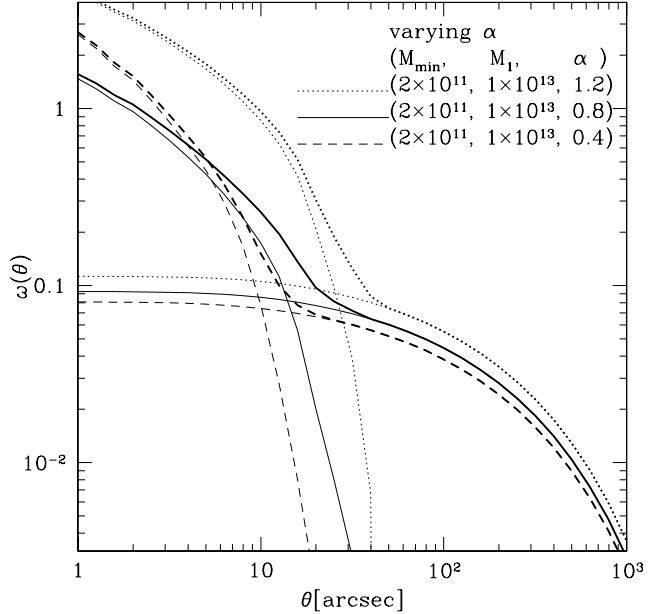


**Figure A3.** Same as Figure A1, but for  $\alpha$ .

halo term. The change in the slope of the 1-halo term with varying  $\alpha$  is explained as follows: Since, roughly speaking, galaxies in larger halos contribute to the 1-halo term on relatively larger scales, while galaxies in smaller halos can only contribute to the 1-halo term on smaller scales. Varying  $\alpha$  changes the fraction in the contribution from larger halos to smaller mass halos, and accordingly changes the slope of the 1-halo term. A smaller  $\alpha$  results a steeper slope, because of a more weight for galaxies in smaller halos.